C-terminal RRM/ACT domain is crucial for fine-tuning the activation of 'long' RelA-SpoT Homolog enzymes by ribosomal complexes

Hiraku Takada[1,2,*], Mohammad Roghanian[1,2], Ievgen Dzhygyr[1,2], Rikinori Murayama[3], Genki Akanuma[4], Gemma C. Atkinson[1], Abel Garcia-Pino[5,6], Vasili Hauryliuk[1,2,7*]

[1]Department of Molecular Biology, Umeå University, Umeå, Sweden

[2]Laboratory for Molecular Infection Medicine Sweden (MIMS), Umeå University, Umeå, Sweden

[3]Akita Prefectural Research Center for Public Health and Environment, 6-6 Senshu-Kubotamachi, Akita, 010-0874, Japan

[4]Department of Life Science, Graduate School of Science, Gakushuin University, Tokyo, Japan

[5]Cellular and Molecular Microbiology, Faculté des Sciences, Université Libre de Bruxelles (ULB), Building BC, Room 1C4 203, Boulevard du Triomphe, 1050, Brussels, Belgium

[6]WELBIO, Avenue Hippocrate 75, 1200 Brussels, Belgium

[7]University of Tartu, Institute of Technology, 50411 Tartu, Estonia

*** Correspondence:**
Hiraku Takada
hiraku.takada@umu.se
Vasili Hauryliuk
vasili.hauryliuk@umu.se

Keywords: ppGpp[1], Rel[2], ACT[3], RRM[4], stringent response[5], ribosome[6]

Abstract

The (p)ppGpp-mediated stringent response is a bacterial stress response implicated in virulence and antibiotic tolerance. Both synthesis and degradation of the (p)ppGpp alarmone nucleotide are mediated by RelA-SpoT Homolog (RSH) enzymes which can be broadly divided in two classes: single-domain 'short' RSHs and multi-domain 'long' RSHs enzymes. The regulatory ACT (Aspartokinase, Chorismate mutase and TyrA) / RRM (RNA Recognition Motif) domain is a near-universal C-terminal domain of long RSHs. Deletion of RRM in both monofunctional (synthesis-only) RelA as well as bifunctional (i.e. capable of both degrading and synthesising the alarmone) Rel renders the long RSH cytotoxic due to overproduction of (p)ppGpp. To probe the molecular mechanism underlying this effect we characterised *Escherichia coli* RelA and *Bacillus subtilis* Rel RSHs lacking RRM. We demonstrate that, first, the cytotoxicity caused by the removal of RRM is counteracted by secondary mutations that disrupt the interaction of the RSH with the starved ribosomal complex – the ultimate inducer of (p)ppGpp production by RelA and Rel – and, second, that the hydrolytic activity of Rel is not abrogated in the truncated mutant. Therefore, we conclude that the overproduction of (p)ppGpp by RSHs lacking the RRM domain is not explained by lack of auto-inhibition in the absence of RRM or/and a defect in (p)ppGpp hydrolysis. Instead, we argue that it is driven by misregulation of the RSH activation by the ribosome.

1 Introduction

Bacteria employ diverse mechanisms to sense and respond to stress. One such mechanism is the stringent response – a near-universal stress response orchestrated by hyper-phosphorylated derivatives of housekeeping nucleotides GDP and GTP: guanosine tetraphosphate (ppGpp) and guanosine pentaphosphate (pppGpp), collectively referred to as (p)ppGpp (Hauryliuk et al., 2015;Liu et al., 2015;Steinchen and Bange, 2016). Since the stringent response and (p)ppGpp-mediated signalling are implicated in virulence, antibiotic resistance and tolerance (Dalebroux et al., 2010;Dalebroux and Swanson, 2012;Hauryliuk et al., 2015), this stress signalling system has been recently targeted for development of new anti-infective compounds (Kushwaha et al., 2019).

Both synthesis and degradation of (p)ppGpp is mediated by RelA/SpoT Homolog (RSH) enzymes. RSHs can be broadly divided into two classes: 'long' multi-domain and 'short' single-domain factors (Atkinson et al., 2011;Jimmy et al., 2019). In the majority of bacteria, including model Gram-positive bacterial species *Bacillus subtilis*, the long multi-domain RSHs are represented by one bifunctional enzyme, Rel (Mittenhuber, 2001;Atkinson et al., 2011). Beta- and gammaproteobacteria, such as *Escherichia coli*, encode two long RSH factors – RelA and SpoT – which are the products of gene duplication and diversification of the ancestral *rel* stringent factor (Mittenhuber, 2001;Atkinson et al., 2011;Hauryliuk et al., 2015). *E. coli* RelA is the most well-studied long RSH. RelA is a dedicated sensor of amino acid starvation with strong (p)ppGpp synthesis activity that is induced by ribosomal complexes harbouring cognate deacylated tRNA in the A-site, so-called 'starved' ribosomal complexes (Haseltine and Block, 1973). Unlike RelA, which lacks (p)ppGpp hydrolysis activity (Shyp et al., 2012), Rel and SpoT can both synthesise and degrade (p)ppGpp (Xiao et al., 1991;Avarbock et al., 2000). Similarly to RelA, (p)ppGpp synthesis by Rel is strongly activated by starved ribosomes (Avarbock et al., 2000). In addition to long RSHs, bacteria often encode single domain RSH enzymes: Small Alarmone Synthetases (SAS) and Small Alarmone Hydrolases (SAS) (Atkinson et al., 2011;Jimmy et al., 2019), such as RelQ and RelP in the Firmicute bacterium *B. subtilis* (Nanamiya et al., 2008).

Long RSHs are universally comprised of two functional regions: the catalytic N-terminal domains (NTD) and the regulatory C-terminal domains (CTD) (**Figure 1A**) (Atkinson et al., 2011). The NTD region comprises the (p)ppGpp hydrolase domain (HD; enzymatically inactive in RelA) and the (p)ppGpp synthetase domain (SYNTH) linked by an α-helical region that regulates the allosteric crosstalk between both domains (Tamman et al., 2019). The CTD encompasses four domains: the Thr-tRNA synthetase, GTPase and SpoT domain (TGS), the Helical domain, the Zing Finger Domain (ZFD) (equivalent to Ribosome-InterSubunit domain, RIS, as per (Loveland et al., 2016), or Conserved Cysteine, CC, as per (Atkinson et al., 2011)), and, finally, the RNA Recognition Motif domain (RRM) (equivalent to Aspartokinase, Chorismate mutase and TyrA, ACT, as per (Atkinson et al., 2011)). When RelA/Rel is bound to a starved ribosomal complex, the TGS domain inspects the deacylated tRNA in the A-site and the TGS domain interacts directly with the 3' CCA end of the A-site tRNA (Arenz et al., 2016;Brown et al., 2016;Loveland et al., 2016). The conserved histidine 432 residue of *E. coli* RelA mediating this interaction is crucial for activation of RelA's enzymatic activity by the 3' CCA (Winther et al., 2018). Both ZFD and RRM interact with the A-site finger (ASF) of the 23S ribosomal RNA (Arenz et al., 2016;Brown et al., 2016;Loveland et al., 2016), and in *E. coli* RelA this contact is crucial for efficient recruitment to and activation by starved ribosomal complexes (Kudrin et al., 2018).

While the NTD is responsible for the enzymatic function of RSHs, the CTD senses the starved ribosomal complex and transmits the signal to activate NTD-mediated (p)ppGpp synthesis by Rel /

84 RelA (Agirrezabala et al., 2013;Arenz et al., 2016;Brown et al., 2016;Loveland et al., 2016). Since
85 removal of the CTD increases the rate of (p)ppGpp production by Rel/RelA in the absence of
86 ribosomes or starved complexes, the CTD was proposed to mediate the auto-inhibition of the NTD
87 synthetase activity, thus precluding uncontrolled production of cytotoxic (p)ppGpp (Schreiber et al.,
88 1991;Gropp et al., 2001;Mechold et al., 2002;Avarbock et al., 2005;Jiang et al., 2007;Yang et al.,
89 2019).

90 The specific focus of this study is the C-terminal RRM / ACT domain of ribosome-associated RSH
91 RelA and Rel. The RRM is absent in RelA enzymes from *Methylotenera mobilitas, Elusimicrobium*
92 *minutum*, *Francisella philomiraga* and *Francisella tularensis* (Atkinson et al., 2011). The only
93 experimentally characterised representative amongst these is *F. tularensis* RelA (Wilkinson et al.,
94 2015). In a reconstituted biochemical system, the factor behaves similarly to *E. coli* RelA, i.e. it has
95 very low synthesis activity by itself – which suggests that the factor is capable of efficient auto-
96 inhibition mechanism – and is potently activated by the ribosome. Conversely, deletion of the RRM
97 domain in factors that naturally possess it leads to over-production of (p)ppGpp in the cell, as shown
98 for *Caulobacter crescentus* (Ronneau et al., 2018) and *Staphylococcus aureus* (Gratani et al., 2018)
99 Rel, as well as *E. coli* RelA (Turnbull et al., 2019). The exact molecular mechanism of misregulation
100 remains unclear, and as a possible explanation it was suggested that the ΔRRM factors overproduce
101 (p)ppGpp due to a lack of auto-inhibition or/and – in the case of *C. crescentus* Rel (Ronneau et al.,
102 2018) – reduced hydrolysis activity.

103 In this report, we inspected the possible role of the ribosome in hyper-activation of ΔRRM variants of
104 long RSHs in the cell. By characterising ΔRRM versions of *E. coli* RelA and *B. subtilis* Rel, we
105 demonstrate that the cytotoxicity of the mutant protein is strictly dependent on the interaction with
106 the ribosome and deacylated tRNA and, therefore, cannot be explained by a lack of autoinhibition
107 alone.

108 2 Materials and Methods

109 2.1 Construction of bacterial strains and plasmids

110 The strains and plasmids used in this study are listed in **Supplementary Tables 1-3**.
111 Oligonucleotides used in this study are provided in **Supplementary Table 4**. A detailed description
112 of strain construction is provided in the *Supplementary Material*.

113 2.2 *E. coli* growth assays

114 *E. coli* BW25113 cells were transformed with expression constructs based on a low copy IPTG
115 inducible vector pNDM220: pNDM220::*relA*, pNDM220::$relA^{\Delta RRM}$, pNDM220::$relA^{\Delta RRM\text{-}H432E}$,
116 pNDM220::$relA^{\Delta RRM\text{-}R629E}$ or pNDM220::$relA^{\Delta RRM\text{-}C612A/C613A}$. For solid medium growth assays, ten-
117 fold serial dilutions of overnight LB cultures were spotted onto LB agar supplemented with 30
118 µg/mL ampicillin and 1 mM IPTG. For liquid medium growth assays, thousand-fold dilutions of the
119 of overnight LB cultures were made in liquid LB supplemented with 30 µg/mL ampicillin and 1 mM
120 IPTG, seeded on a 100-well honeycomb plate (Oy Growth Curves AB Ltd, Helsinki, Finland), and
121 plates incubated in a Bioscreen C (Labsystems, Helsinki, Finland) at 37 °C with continuous medium
122 shaking.

123 2.3 Preparation of polyclonal anti-Rel antiserum

124 The entire coding region of the *B. subtilis rel* gene was amplified by PCR using the synthetic
125 oligonucleotide pQErelA_F and pQErelA_R containing a BamHI site and *B. subtilis* genomic DNA
126 as a template. The resulting PCR fragment was cut with BamHI and then inserted into the BamHI
127 sites of pQE60 (Qiagen), yielding plasmid pQErelA. pOErelA was transformed into *E. coli* M15
128 (pREP4) (Qiagen), fresh transformants were inoculated into LB liquid culture (1000 mL) with 100
129 µg/mL ampicillin and grown at 37 °C with vigorous shaking. At OD_{600} of 0.8 expression of Rel
130 induced with 1 mM IPTG (final concentration). After 3 hours of expression the cells were harvested
131 by centrifugation, resuspended in buffer A (500 mM NaCl, 50 mM Tris-HCl pH 8.0) supplemented
132 with 2 mM PMSF and lysed by sonication. Rel-His_6 inclusion bodies were collected by
133 centrifugation, resuspended in buffer A supplemented with 8 M guanidine hydrochloride (= buffer B)
134 and loaded onto an Ni-NTA agarose column (QIAGEN) pre-equilibrated in the same buffer. The
135 column was washed with buffer B supplemented with 10 mM imidazole, and the protein was eluted
136 with a 100-400 mM imidazole gradient in buffer B. The fractions containing Rel-His_6 was dialyzed
137 against buffer A at 4 °C overnight. Aggregated Rel-His_6 protein was collected by centrifugation,
138 resuspended in buffer A supplemented with 6 M urea and used for rabbit immunization. Rabbit
139 serum was used as a polyclonal anti-Rel antibody.

140 **2.4 Sucrose gradient fractionation and Western blotting**

141 *B. subtilis* strains were pre-grown on LB plates overnight at 30 °C. Fresh individual colonies were
142 used to inoculate 200 mL LB cultures that were grown at 37 °C. At OD_{600} of 0.2 amino acid
143 starvation was induced by addition of isoleucyl tRNA synthetase inhibitor mupirocin (dissolved in
144 DMSO, AppliChem) to final concentration of 700 nM for 20 minutes. As a mock control, a separate
145 culture was treated with the same amount of DMSO. After 20 minutes the cells were collected by
146 centrifugation (8,000 rpm, 5 minutes, JLA-16.25 Beckman Coulter rotor), dissolved in 0.5 mL of
147 HEPES:Polymix buffer (5 mM $Mg(OAc)_2$) supplemented with 2 mM PMSF, lysed using FastPrep
148 homogenizer (MP Biomedicals) by four 20 seconds pulses at speed 6.0 mp/sec with chilling on ice
149 for 1 minutes between the cycles), and clarified by ultracentrifugation (14,800 rpm for 20 minutes,
150 Microfuge 22R centrifuge Beckman Coulter, F241.5P rotor).

151 For Western blotting 0.5 mL fractions were supplemented with 1.5 mL of 99.5% ethanol, precipitated
152 overnight at –20 °C. After centrifugation at 14,800 rpm for 30 minutes at 4 °C the supernatants were
153 discarded and the samples were dried. The pellets were resuspended in 40 µL of 2xSDS loading
154 buffer (100 mM Tris-HCl pH 6.8, 4% SDS (w/v) 0.02% Bromophenol blue, 20% glycerol (w/v) 4%
155 β-mercaptoethanol), resolved on the 12% SDS PAGE and transferred to nitrocellulose membrane
156 (Trans-Blot Turbo Midi Nitrocellulose Transfer Pack, Bio-Rad , 0.2 µm pore size) with the use of a
157 Trans-Blot Turbo Transfer Starter System (Bio-Rad) (10 minutes, 2.5A, 25V). Membrane blocking
158 was done for one hour in PBS-T (1xPBS 0.05% Tween-20) with 5% w/v nonfat dry milk at room
159 temperature. Rel was detected using either anti-Rel primary combined with goat anti-rabbit IgG-HRP
160 secondary antibodies or anti-L3 primary antibodies (a gift from Fujio Kawamura (Murina et al.,
161 2018b)) combined with goat anti-rabbit IgG-HRP secondary antibodies, respectively. All antibodies
162 were used at 1:10,000 dilution. ECL detection was performed using WesternBright™ Quantum (K-
163 12042-D10, Advansta) Western blotting substrate and an ImageQuant LAS 4000 (GE Healthcare)
164 imaging system.

165 **2.5 Expression and purification of *E. coli* RelA and *B. subtilis* Rel**

166 Wild type and H432E mutant variants of *E. coli* RelA were expressed and purified as described
167 earlier (Turnbull et al., 2019).

168 Wild type and mutant variants of *B. subtilis* Rel were overexpressed in freshly transformed *E. coli*
169 BL21 DE3 Rosetta (Novagen). Fresh transformants were inoculated to final OD_{600} of 0.05 in the LB
170 medium (800 mL) supplemented with 100 µg/mL kanamycin. The cultures were grown at 37 °C until
171 an OD_{600} of 0.5, induced with 1 mM IPTG (final concentration) and grown for additional 1.5 hour at
172 30 °C. The cells were harvested by centrifugation and resuspended in buffer A (750 mM KCl, 5 mM
173 $MgCl_2$, 40 µM $MnCl_2$, 40 µM $Zn(OAc)_2$, 1 mM mellitic acid (Tokyo Kasei Kogyo Co., Ltd.), 20
174 mM imidazole, 10% glycerol, 4 mM β-mercaptoethanol, 25 mM HEPES:KOH pH 8) supplemented
175 with 0.1 mM PMSF and 1 U/mL of DNase I. Cells were lysed by one passage through a high-
176 pressure cell disrupter (Stansted Fluid Power, 150 MPa), cell debris was removed by centrifugation
177 (25,000 rpm for 40 min, JA-25.50 Beckman Coulter rotor) and clarified lysate was taken for protein
178 purification.

179 To prevent possible substitution of Zn^{2+} ions in Rel's Zn-finger domain for Ni^{2+} during purification
180 on an Ni-NTA metal affinity chromatography column (Block et al., 2009), a 5 mL HisTrap HP
181 column was stripped from Ni^{2+} in accordance with manufacturer's recommendations, washed with 5
182 column volumes (CV) of 100 mM $Zn(OAc)_2$ pH 5.0 followed by 5 CV of deionized water. Clarified
183 cell lysate was filtered through a 0.2 µm syringe filter and loaded onto the Zn^{2+}-charged HisTrap 5
184 mL HP column pre-equilibrated in buffer A. The column was washed with 5 CV of buffer A, and the
185 protein was eluted with a linear gradient (6 CV, 0-100% buffer B) of buffer B (750 mM KCl, 5 mM
186 $MgCl_2$, 40 µM $MnCl_2$, 40 µM $Zn(OAc)_2$, 1 mM mellitic acid, 500 mM imidazole, 10% glycerol, 4
187 mM β-mercaptoethanol, 25 mM HEPES:KOH pH 8). Mellitic acid forms highly ordered molecular
188 networks when dissolved in water (Inabe, 2005) and it was shown to promote the stability of
189 *Thermus thermophilus* Rel (Van Nerom et al., 2019). Fractions most enriched in Rel (≈25-50% buffer
190 B) were pooled, totalling approximately 5 mL. The sample was loaded on a HiLoad 16/600 Superdex
191 200 pg column pre-equilibrated with a high salt buffer (buffer C; 2 M NaCl, 5 mM $MgCl_2$, 10%
192 glycerol, 4 mM β-mercaptoethanol, 25 mM HEPES:KOH pH 8). The fractions containing Rel were
193 pooled and applied on HiPrep 10/26 desalting column (GE Healthcare) pre-equilibrated with storage
194 buffer (buffer D; 720 mM KCl, 5 mM $MgCl_2$, 50 mM arginine, 50 mM glutamic acid, 10% glycerol,
195 4 mM β-mercaptoethanol, 25 mM HEPES:KOH pH 8). Arginine and glutamic acid were added to
196 improve protein solubility and long-term stability (Golovanov et al., 2004). The fractions containing
197 Rel were collected and concentrated in an Amicon Ultra (Millipore) centrifugal filter device (cut-off
198 50 kDa). To cleave off the His_{10}-SUMO tag, 35 µg of His_6-Ulp1 per 1 mg of Rel were added and the
199 reaction mixture was incubated at room temperature for 15 min. After the His_{10}-SUMO tag was
200 cleaved off, the protein was passed though 5 mL Zn^{2+}-charged HisTrap HP pre-equilibrated with
201 buffer D. Fractions containing Rel in the flow-through were collected and concentrated on Amicon
202 Ultra (Millipore) centrifugal filter device with 50 kDa cut-off. The purity of protein preparations was
203 assessed by SDS-PAGE and spectrophotometrically (OD_{260}/OD_{280} ratio below 0.8 corresponding to
204 less than 5% RNA contamination (Layne, 1957)). Protein preparations were aliquoted, frozen in
205 liquid nitrogen and stored at –80 °C. Individual single-use aliquots were discarded after the
206 experiment. Chromatography profiles and the corresponding SDS-PAGE gels for wild type Rel
207 purification as well as gel filtration profiles for ΔRRM mutant Rel variant are presented on (**Figure**
208 **2**).

209 **2.6 Preparation of 10X Polymix buffer base**

210 The 10X Polymix base was prepared as per (Antoun et al., 2004), with minor modifications. For
211 preparation of the putrescine solution, 100 g of putrescine (1,4-diaminobutane) was dissolved in 600
212 mL of ddH_2O at 90 °C, and the pH adjusted with acetic acid to 8.0 (approximately 100 mL of 100%
213 acetic acid). After cooling to room temperature, the pH was adjusted further to 7.6 and the volume

214 was adjusted to the final of 2 L by addition of 1.134 L of ddH_2O. One 100 mL cup of activated
215 charcoal was added and the slurry was stirred under the hood for 30 minutes. The slurry was filtered
216 through, first, Whatman paper and then through a 0.45 µm BA85 membrane. The final solution was
217 stored at 4 °C in a bottle wrapped in foil since putrescine is photosensitive. The preparation of 2 L of
218 10X Polymix buffer base used 141.66 g KCl, 5.35 g NH_4Cl, 21.44 g $Mg(OAc)_2 \bullet 4H_2O$, 1.47 g
219 $CaCl_2 \bullet 2H_2O$, 5.092 g spermidine, and 160 ml of putrescine solution (described above). The salts
220 were dissolved in ddH_2O (≈1,500 mL), then the putrescine solution was added and mixed well.
221 Spermidine was dissolved in a small volume of ddH_2O and added to the mixture. The pH was
222 adjusted to 7.5 with concentrated acetic acid or 5 M KOH, and after that the volume was adjusted by
223 adding ddH_2O to 2 L. The buffer was filtered through 0.2 µm nitrocellulose filter (2-3 filters are
224 needed). The resulting 10X Polymix buffer base was aliquoted and stored at –20 °C. The final
225 working HEPES:Polymix buffer was made using the 10X Polymix buffer base, 1M DDT and 1 M
226 HEPES:KOH pH 7.5 and contains 20 mM HEPES:KOH pH 7.5, 2 mM DTT, 5 mM $MgOAc_2$, 95
227 mM KCl, 5 mM NH_4Cl, 0.5 mM $CaCl_2$, 8 mM putrescine, 1 mM spermidine.

228 **2.7 Purification of *B. subtilis* 70S ribosomes**

229 *B. subtilis* strain RIK2508 (*trpC2* Δ*hpf*) strain (Akanuma et al., 2016;Brodiazhenko et al., 2018) was
230 pre-grown on LB plates overnight at 30 °C. Fresh individual colonies were used to inoculate LB
231 liquid cultures (25 × 400 mL) to OD_{600} of 0.05 and grown at 37 °C with vigorous shaking. At OD_{600}
232 1.2 the cells were pelleted at 4 °C (TLA10.500 (Beckman), 15 min at 5,000-8,000 rcf), resuspended
233 with ice-cold PBS buffer, pelleted again in 50 mL Falcon tubes, frozen with liquid nitrogen and
234 stored at –80 °C. Approximately 20 g of frozen *B. subtilis* cells were resuspended in 50 mL of cell
235 opening buffer (100 mM NH_4Cl, 15 mM $Mg(OAc)_2$, 0.5 mM EDTA, 3 mM β-mercaptoethanol, 20
236 mM Tris:HCl pH 7.5) supplemented with 1 mU Turbo DNase (Thermo Fisher Scientific), 0.1 mM
237 PMSF and 35 µg/mL lysozyme, incubated on ice for one hour, and opened by three passages on a
238 high-pressure cell disrupter (Stansted Fluid Power) at 220 MPa. Lysed cells were clarified by
239 centrifugation for 40 min at 40,000 rpm (Ti 45 rotor, Beckman), NH_4Cl concentration was adjusted
240 to 400 mM, and the mixture was filtered through 0.45 µm syringe filters. The filtrated lysate was
241 loaded onto a pre-equilibrated 80 mL CIMmultus QA-80 column (BIA Separations, quaternary
242 amine advanced composite column) at a flow rate of 20 mL/min, and the column washed with 5 CV
243 (CV = 80 mL) of low salt buffer (400 mM NH_4Cl, 15 mM $Mg(OAc)_2$, 3 mM β-mercaptoethanol, 20
244 mM Tris:HCl pH 7.5). Ribosomes were then eluted in 45 mL fractions by a step gradient to 77% high
245 salt buffer (900 mM NH_4Cl, 15 mM $Mg(OAc)_2$, 3 mM β-mercaptoethanol, 20 mM Tris:HCl pH 7.5)
246 for 5 CV, followed by 100% high salt buffer for 1 CV. The fractions containing ribosomes were
247 pooled, the concentration of NH_4Cl was adjusted to 100 mM, and the ribosomes were treated with
248 puromycin added to a final concentration of 10 µM. The resultant crude 70S preparation was
249 resolved on a 10-40% sucrose gradient in overlay buffer (60 mM NH_4Cl, 15 mM $Mg(OAc)_2$, 0.25
250 mM EDTA, 3 mM β-mercaptoethanol, 20 mM Tris:HCl pH 7.5) in a zonal rotor (Ti 15, Beckman, 17
251 hours at 21,000 rpm). The peak containing pure 70S ribosomes was pelleted by centrifugation (20
252 hours at 35,000 rpm), and the final ribosomal preparation was dissolved in HEPES:Polymix buffer
253 (20 mM HEPES:KOH pH 7.5, 2 mM DTT, 5 mM $Mg(OAc)_2$, 95 mM KCl, 5 mM NH_4Cl, 0.5 mM
254 $CaCl_2$, 8 mM putrescine, 1 mM spermidine (Antoun et al., 2004)). 70S concentration was measured
255 spectrophotometrically (1 OD_{260} corresponds to 23 nM of 70S) and ribosomes were aliquoted (50-
256 100 µL per aliquot), snap-frozen in liquid nitrogen and stored at –80 °C.

257 **2.8 Preparation of 70S initiation complexes (70S IC)**

258 Initiation complexes were prepared by as per (Murina et al., 2018a), with minor modifications. The

reaction mix containing *B. subtilis* 70S ribosomes (final concentration of 6 μM) with *E. coli* IF1 (4 μM), IF2 (5 μM), IF3 (4 μM), ^{3}H-fMet-tRNA$_{i}^{fMet}$ (8 μM), mRNA MVFStop (8 μM, 5'-GGC**AAGGAGGA**GAUAAGAAUGGUUUUCUAAUA-3'; Shine-Dalgarno sequence is highlighted in bold, ORF is underlined), 1 mM GTP and 2 mM DTT in 1×HEPES:Polymix buffer (20 mM HEPES:KOH pH 7.5, 95 mM KCl, 5 mM NH_4Cl, 5 mM $Mg(OAc)_2$, 0.5 mM $CaCl_2$, 8 mM putrescine, 1 mM spermidine, 1 mM DTT (Antoun et al., 2004)) was incubated at 37 °C for 30 min. Then the ribosomes were pelleted through a sucrose cushion (1.1 M sucrose in HEPES:Polymix buffer with 15 mM Mg^{2+}) at 50,000 rpm for two hours (TLS-55, Beckman), the pellet was dissolved in HEPES:Polymix buffer (5 mM $Mg(OAc)_2$), aliquoted, frozen in liquid nitrogen and stored at –80 °C.

2.9 Preparation of ^{3}H-labelled pppGpp

3 μM *E. fecalis* RelQ (Beljantseva et al., 2017) were incubated in reaction buffer (18 mM $MgCl_2$, 20 mM DTT, 20 M Tris-HCl pH 8.0) together with 8 mM ATP and 5 mM ^{3}H-GTP (SA: 100 cpm/pmol) for 2 hours at 37 °C to produce ^{3}H-pppGpp. The resultant mixture was loaded on strong anion-exchange column (MonoQ 5/50 GL; GE Healthcare), and nucleotides were resolved by a 0.5-1,000 mM LiCl gradient. Peak fractions containing ^{3}H-pppGpp were pooled and precipitated by addition of lithium chloride to a final concentration of 1 M followed by addition of four volumes of ethanol. The suspension was incubated at –80 °C overnight and centrifuged (14,800 rpm, 30 min, 4 °C). The resulting pellets were washed with absolute ethanol, dried, dissolved in 20 mM HEPES-KOH buffer (pH 7.5) and stored at –80 °C.

2.10 ^{3}H-pppGpp hydrolysis assay

The reaction mixtures contained 140-250 nM Rel, 300 μM ^{3}H-pppGpp, 1 mM $MnCl_2$, an essential cofactor for Rel's hydrolysis activity (Avarbock et al., 2000;Mechold et al., 2002;Tamman et al., 2019), all in HEPES:Polymix buffer (5 mM Mg^{2+} final concentration). After preincubation at 37 °C for 3 minutes, the reaction was started by the addition of prewarmed Rel and 5 μL aliquots were taken throughout the time course of the reaction and quenched with 4 μL 70% formic acid supplemented with a cold nucleotide standard (4 mM GDP and 4 mM GTP) for UV-shadowing.

2.11 ^{3}H-pppGpp synthesis assay

Assays with *E. coli* RelA were performed as described earlier (Kudrin et al., 2018). In the case of *B. subtilis* RelA, the reaction mixtures typically contained 500 nM *B. subtilis* 70S IC(MVF), 140 nM Rel, guanosine nucleoside substrate (300 μM ^{3}H-GTP, PerkinElmer), 100 μM pppGpp, 2 μM *E. coli* tRNA^{Val} (Chemical Block), all in HEPES:Polymix buffer (5 mM Mg^{2+} final concentration). After preincubation at 37 °C for 3 minutes, the reaction was started by the addition of prewarmed ATP to the final concentration of 1 mM, and 5 μL aliquots were taken throughout the time course of the reaction and quenched with 4 μL 70% formic acid supplemented with a cold nucleotide standard (4 mM GDP and 4 mM GTP) for UV-shadowing. Individual quenched timepoints were spotted PEI-TLC plates (Macherey-Nagel) and nucleotides were resolved in 0.5 KH_2PO_4 pH 3.5 buffer. The TLC plates were dried, cut into sections as guided by UV-shadowing, and ^{3}H radioactivity was quantified by scintillation counting in EcoLite™ Liquid Scintillation Cocktail (MP Biomedicals).

3 Results

3.1 Toxicity of *E. coli* ΔRRM RelA is countered by mutations compromising the interaction with starved ribosomes

To test whether the toxicity of $RelA^{\Delta RRM}$ in *E. coli* is dependent on the interaction with starved complexes, we used our system for low-level ectopic expression of RelA from a low copy number mini R1 plasmid (pNDM220, present in one to two copies per chromosome (Molin et al., 1979)) under the control of $P_{A1/O4/O3}$ promoter (Turnbull et al., 2019). Guided by the recent cryo-EM reconstructions of RelA (Arenz et al., 2016;Brown et al., 2016;Loveland et al., 2016), we designed a set of mutations that will specifically disrupt RelA's interaction with starved ribosomal complexes.

To disrupt the interaction between RelA and the tRNA, we adopted the H432E mutation in the TGS domain that was earlier shown to specifically abrogate the recognition of the 3' CCA end of the A/R tRNA (Winther et al., 2018). This conserved histidine residue stacks between the two cytosine bases and hydrogen-bonds the phosphodiester backbone (**Figure 1B**). Replacing it with glutamic acid introduces a charge repulsion effect as well as a steric clash. To disrupt the interaction with the ribosome we used mutations in the ZFD: R629E as well as a double substitution C602A/C603A; both mutants are expected to compromise the recognition of the 23S rRNA ASF element that is crucial for RelA recruitment (Kudrin et al., 2018). The conserved double motif docks the ZFD α-helix into the major groove of the ASF; replacement by alanine is expected to abrogate this interaction (**Figure 1C**). The conserved arginine 629 residue is in close proximity to A886-A887 and A885-A886 phosphodiester bonds (3.5Å and 5Å, respectively), and, therefore, the R629E substitution is expected to cause electrostatic repulsion.

In good agreement with our previous results (Turnbull et al., 2019), low-level expression of full-length RelA has a minor, but detectable growth inhibitory effect both when tested on solid Agar media (**Figure 3A**) and in liquid LB cultures (growth rate decreases from 60 (vector) to 89 min) (**Figure 3B**). Deletion of the RRM renders RelA significantly more toxic (growth rate decreases to 148 min). The effect is countered by TGS H432E, ZFD R629E and even more so by the C612A/C613A mutations (**Figure 3AB**). We directly confirm the lack of activation by deacylated tRNA in the case of H432E *E. coli* RelA using biochemical assays (**Supplementary Figure 1**).

Taken together, our results suggest that $RelA^{\Delta RRM}$ toxicity in *E. coli* could be dependent on the interaction with starved ribosomes and is not due to a defect in auto-inhibition alone. To test the generality of this hypothesis, we next characterised *B. subtilis* Rel lacking the RRM domain.

3.2 Toxicity of *B. subtilis* ΔRRM Rel is mediated by (p)ppGpp synthesis and is countered by mutations compromising the interaction with starved ribosomes

We expressed ΔRRM Rel under the control of an IPTG-inducible $P_{hy\text{-}spank}$ promotor (Britton et al., 2002) in $ppGpp^0$ (Δ*rel*Δ*relP*Δ*relQ*) (Nanamiya et al., 2008) or Δ*rel B. subtilis* strains (**Figure 4A**). In the $ppGpp^0$ background, inhibition of *B. subtilis* growth on LB plates is a marker of toxic (p)ppGpp overproduction. In the Δ*rel* background (p)ppGpp is overproduced by a SAS in the absence of Rel's hydrolytic activity, causing a growth defect in *B. subtilis* (Nanamiya et al., 2008) and *S. aureus* (Geiger et al., 2014). Therefore, this experiment tests the complementation of hydrolase function of Rel that manifests in improved growth.

Unlike the full-length Rel, the $Rel^{\Delta RRM}$ truncation is toxic in the $ppGpp^0$ and Δ*rel* backgrounds, both when the growth is followed on plates (**Figure 4A**) and in liquid culture (**Figure 4BC**). To probe the role of the interactions with starved ribosomes in $Rel^{\Delta RRM}$ toxicity, we used a set of substitutions in *B. subtilis* RelA corresponding to those used to study *E. coli* RelA (**Figures 1** and **3**). The toxicity of

343 the $Rel^{\Delta RRM}$ mutant is efficiently countered by the H420E substitution in the TGS as well as the
344 R619E and C602A/C603A substitutions in the ZFD (**Figure 4D**). This strongly suggests that the
345 intact interaction with tRNA and starved ribosomes is essential for the toxicity of $Rel^{\Delta RRM}$. For
346 comparison, we tested, full-length Rel, $Rel^{\Delta RRM\Delta ZDF}$ C-terminal truncation, as well as the NTD
347 domain region alone. The $Rel^{\Delta RRM\Delta ZDF}$ mutant is only slightly toxic in the $ppGpp^0$ background and its
348 expression promotes growth in the Δ*rel* background (**Figure 4A**). NTD-alone construct displays no
349 toxicity in the $ppGpp^0$ background and does not promote the growth in the Δ*rel* background,
350 suggesting weak – or absent – synthetase activity.

351 To separate the effects of (p)ppGpp production from the effects of (p)ppGpp degradation, we tested
352 synthesis-deficient SYNTH D264G mutants (Nanamiya et al., 2008) of C-terminally truncated Rel
353 variants (**Figure 4A**). The toxicity of the ΔRRM variant is abolished by the D264G mutation
354 demonstrating that it is, indeed, mediated by (p)ppGpp production and not, for example, through
355 inhibition of protein synthesis via competitive binding to ribosomal A-site (the latter non-enzymatic
356 mechanism of toxicity was shown for *E. coli* $RelA^{CTD}$ (Turnbull et al., 2019)). Both ΔRRM D264G
357 and ΔZFDΔRRM D264G variants promote growth in the Δ*rel* strain suggesting that neither deletion
358 of ΔRRM alone – or both ΔZFD and ΔRRM – abrogates the hydrolysis activity of *B. subtilis* Rel
359 (**Figure 4A**, bottom panel). At the same time expression of the synthesis-inactive D264G Rel^{NTD} has
360 no effect, suggesting that the NTD does not efficiently hydrolyse (p)ppGpp. To test if further
361 truncations of the NTD-only Rel (Rel^{1-373}) would induce hydrolytic activity, we tested several
362 additional constructs of *B. subtilis* Rel – Rel^{1-336}, Rel^{1-196} and Rel^{155} – but neither of them could
363 rescue the growth effect of Δ*rel B. subtilis* (**Supplementary Figure S2**).

364 Taken together, our results demonstrate that i) $Rel^{\Delta RRM}$ is toxic in *B. subtilis,* ii) the toxicity is
365 mediated by (p)ppGpp synthesis and iii) it is abrogated by mutations disrupting the interaction with
366 tRNA and starved ribosomes. This suggests that the misactivation of the $Rel^{\Delta RRM}$ mutant by the
367 ribosome is the underlying cause of the toxicity.

368 3.3 Expression of $Rel^{\Delta RRM}$, $Rel^{\Delta RRM\Delta ZFD}$ and Rel^{NTD} but not Rel^{H420E} TGS mutant suppresses
369 amino acid auxotrophy of $ppGpp^0$ *B. subtilis*

370 To test the low-level, non-toxic, synthesis activity of Rel mutants and to validate the effects of point
371 mutations disrupting the interaction of Rel with starved ribosomal complexes, we took advantage of
372 the amino acid auxotrophy phenotype of the $ppGpp^0$ *B. subtilis* (Δ*rel*Δ*relP*Δ*relQ*) (Nanamiya et al.,
373 2008)).

374 When $ppGpp^0$ *B. subtilis* is grown on Spizizen minimum medium (Spizizen, 1958) in the absence of
375 casamino acids, neither of the D264G Rel mutants – either full-length or C-terminal truncations –
376 promote growth, both whether or not expression is induced by 1 mM IPTG (**Figure 4E**, right panels).
377 Full induction of NTD expression with 1 mM IPTG near-completely supressed the auxotrophy
378 phenotype (**Figure 4E**, top right panel), while the leaky expression in the absence of IPTG results in
379 weak, but detectable suppression (**Figure 4E**, bottom right panel). This demonstrates that *B. subtilis*
380 NTD has a weak net-synthesis activity. The $Rel^{\Delta RRM}$ is, as expected, highly toxic when expression is
381 induced by IPTG; conversely, low-level leakage expression efficiently supresses the amino acid
382 auxotrophy phenotype. Removal of both RRM and ZFD domains renders the protein non-toxic. It is
383 not trivial to reconcile this effect with the idea that removal of the RRM renders the protein toxic due
384 to lack of auto-inhibition: one would expect that the additional removal of the ZFD domain would
385 further compromise the CTD-mediated negative control in $Rel^{\Delta RRM}$.

386 We next used the auxotrophy assay to test the effects of the H420E TGS and C602A/C603A ZFD
387 substitutions on the activity of Rel expressed from the native genomic locus under the control of the
388 native promotor (**Figure 4F**). As a positive control we used a strain lacking the genomic copy of *relC*
389 encoding ribosomal protein L11. This ribosomal element is essential for *E. coli* RelA activation by
390 starved ribosomal complexes (Parker et al., 1976;Wendrich et al., 2002;Shyp et al., 2012) as well as
391 for cellular functionality of *C. crescentus* Rel (Boutte and Crosson, 2011). The $ppGpp^0$ strain
392 expressing H420E Rel fails to growth on the minimum media, reinforcing the crucial role of that this
393 residue, while the C602A/C603A can sustain the growth, suggesting that this substitution does not
394 completely abrogate the activity.

395 **3.4 RRM deletion and ZFD mutations destabilise *B. subtilis* Rel binding to starved ribosomal**
396 **complexes**

397 Next, we probed the ribosomal association of ΔRRM and full-length Rel expressed in the $ppGpp^0$
398 background using a centrifugation sucrose gradient followed by Western blotting using antiserum
399 against native, untagged *B. subtilis* Rel (**Figure 5A**). Since deacylated tRNA promotes ribosomal
400 recruitment of *E. coli* RelA (Agirrezabala et al., 2013;Kudrin et al., 2017), we probed the association
401 of wild type and mutant Rel variants with the ribosome both under exponential growth and upon
402 acute isoleucine starvation induced by the isoleucyl tRNA synthetase inhibitor antibiotic mupirocin
403 (pseudomonic acid) (Thomas et al., 2010). In good agreement with the cryo-EM structures detailing
404 multiple contacts between the RRM and the starved complex and therefore suggesting an importance
405 of this element in ribosomal recruitment (Arenz et al., 2016;Brown et al., 2016;Loveland et al.,
406 2016), we do not detect a stable association of ΔRRM Rel with the ribosome upon a mupirocin
407 challenge. This suggests that the interaction with the ribosome is significantly destabilised in $Rel^{\Delta RRM}$
408 and the protein dissociates during centrifugation. It is noteworthy that, despite an unstable association
409 of $Rel^{\Delta RRM}$ with starved ribosomes, the expression of this protein strongly induces the accumulation
410 of 100S ribosomal dimers, which is indicative of (p)ppGpp overproduction (Tagami et al., 2012).

411 Our microbiological experiments demonstrate that both the C602A and C603A double substitution
412 and the R619E point substitution render $Rel^{\Delta RRM}$ non-toxic, which we attribute to further
413 destabilisation of Rel's interaction with starved ribosomal complexes (**Figure 4D**). To directly probe
414 the effects of these mutations, we used centrifugation experiments with full-length Rel carrying the
415 substitutions. As expected, both the C603A double mutant and R619E full-length variants are
416 compromised in recruitment to the ribosome upon a mupirocin challenge (**Figure 5A**).

417 Taken together, these results demonstrate that $Rel^{\Delta RRM}$ is significantly more toxic (i.e. more active in
418 (p)ppGpp production in the cell) than the full-length protein and this toxicity is dependent on the
419 interaction with starved ribosomes, which is, in turn, destabilised in this truncation. As a next step,
420 we set out to test the effects of RRM deletion – either alone or in combination with mutations further
421 compromising the interactions with starved ribosomes – on Rel's enzymatic activity in a
422 reconstituted *B. subtilis* biochemical system.

423 **3.5 Purification of RNA-free untagged *B. subtilis* Rel requires size-exclusion chromatography**

424 To purify untagged *B. subtilis* Rel we combined our protocols used for purification of *E. coli* RelA
425 (Turnbull et al., 2019) and *T. thermophilus* Rel (Van Nerom et al., 2019). (**Figure 2**). Importantly,
426 during all of the chromatography steps we followed both absorbance at 260 and 280 nm
427 complemented with SDS PAGE analysis of fractions. This is essential in order to identify and
428 specifically pool the fractions containing Rel free from RNA contamination. After the initial capture

429 using immobilized metal affinity chromatography (IMAC) in high ionic strength conditions (750 mM
430 KCl) using HisTrap HP column charged with Zn^{2+} in order to avoid possible replacement of the Zn^{2+}
431 in the ZFD domain by Ni^{2+} ions (Block et al., 2009), His_{10}-SUMO-Rel was applied on size-exclusion
432 chromatography (SEC) on HiLoad 16/600 Superdex 200 pg column (**Figure 2D**). Both in the case of
433 the full length (**Figure 2B**) and ΔRRM Rel (**Figure 2C**), the RNA-free fractions constitute the
434 minority of the protein that elute considerably later than the bulk of the RNA-contaminated Rel
435 which elutes considerably. While the SEC step is essential for generating RNA-free Rel preparations,
436 the majority of the protein prep is lost at this stage. After the SEC step, the buffer was exchanged to
437 storage buffer containing arginine and glutamic acid that improve protein solubility and long-term
438 stability (Golovanov et al., 2004) (**Figure 2D**), His_{10}-SUMO tag was cleaved off and removed by
439 passing the protein via second IMAC (**Figure 2E**). The quality of the final preparations was assessed
440 by SDS-PAGE (**Figure 2F**) as well as spectrophotometrically: OD_{260}/OD_{280} ratio below 0.8
441 corresponding to less than 5% RNA contamination (Layne, 1957).

442 **3.6 The RRM deletion does not abrogate the hydrolysis activity of *B. subtilis* Rel**

443 It was recently proposed that the RRM domain has a stimulatory effect on the hydrolysis activity of
444 *C. crescentus* Rel, and the loss of this regulatory mechanism explains the toxicity of the ΔRRM
445 mutant (Ronneau et al., 2018). This hypothesis does not explain the toxicity of the ΔRRM variant of
446 the synthesis-only RSH RelA (Turnbull et al., 2019) and our microbiological experiments showing
447 that the synthesis-defective ΔRRM D264G variant of *B. subtilis* Rel remains active as a (p)ppGpp
448 hydrolase (**Figure 4A**). Enzymatic assays following ^{3}H-pppGpp degradation by full-length and
449 $Rel^{\Delta RRM}$ show that the latter is approximately twice less active (**Figure 5B**). While the defect is
450 detectable, it is in good agreement with our microbiological experiments, relatively mild.
451 Importantly, the enzyme characterised by Ronneau and colleagues (*C. crescentus* $Rel^{\Delta 668\text{-}719}$) was not
452 completely lacking the RRM, and it is possible that the remaining beta-strand alpha-helix turn
453 structural element was interfering with the hydrolysis activity of the construct (Ronneau et al., 2018).

454 **3.7 The R619E ZFD substitution compromises activation of *B. subtilis* $Rel^{\Delta RRM}$ by starved**
455 **ribosomal complexes**

456 We tested the ^{3}H-pppGpp synthesis by full-length Rel as well as $Rel^{\Delta RRM}$, either alone or activated by
457 the ribosomes or starved complexes in a reconstituted system (**Figure 5C**). When the protein is tested
458 by itself, the $Rel^{\Delta RRM}$ mutant is less active than the full-length, suggesting that deletion of the RRM
459 domain does not lead to the loss of auto-inhibition. While $Rel^{\Delta RRM}$ remains less active than the full-
460 length when activated by initiation complexes (about two-fold), in the presence of starved ribosomal
461 complexes the two proteins are equally active. This could be explained by tRNA stabilising Rel on
462 the ribosome and overriding the defect caused by the removal of the RRM domain.

463 The R619E mutation compromises activation of the full-length Rel by the initiation complexes (more
464 than four-fold), and the effect is less pronounced in the presence of deacylated $tRNA^{Val}$ (less than
465 two-fold decrease in activity). Just as in the case of the RRM deletion, a possible explanation is that
466 the deacylated tRNA strongly stimulates the binding of Rel to the ribosome and offsets the effect of
467 the mutation R619E. When the R619E substitution is introduced into ΔRRM Rel, the combination of
468 the two mutations destabilising Rel binding to the ribosome results in compromised activation both
469 by the initiation (five-fold) and starved (seven-fold) ribosomal complex. Despite several attempts we
470 failed to generate sufficiently pure and soluble C602/C603 $Rel^{\Delta RRM}$, which precluded direct
471 biochemical characterisation of this mutant.

472 Taken together, our biochemical results demonstrate that while RRM is important in Rel recruitment
473 to the ribosome, this domain is not absolutely essential for the activation of its (p)ppGpp synthesis
474 activity by starved ribosomal complexes, which is consistent with the ribosome-dependent nature of
475 the Rel$^{\Delta RRM}$ toxicity in live cells.

476 **4 Discussion**

477 Taken together, our results demonstrate that i) deletion of the RRM domain renders *B. subtilis* Rel
478 and *E. coli* RelA toxic due to (p)ppGpp overproduction in a ribosome and tRNA-dependent manner,
479 ii) RRM deletion does not abrogate the (p)ppGpp hydrolysis activity of *B. subtilis* Rel iii) RRM
480 deletion destabilises the interaction of *B. subtilis* Rel with starved ribosomal complexes, and iv) this
481 destabilisation renders the mutant enzyme more sensitive than the full length Rel to deactivation by
482 additional substitutions further compromising its association with starved ribosomes. Our
483 biochemical results do not explain why exactly ΔRRM Rel/RelA is toxic: if anything, the protein
484 behaves as a poorer binder (**Figure 3D**) and is less active (**Figure 3E**) as compared to the full-length
485 Rel. A dedicated follow-up study is necessary to clarify this question.

486 Our report expands the mutation toolbox for dissecting the molecular mechanisms of long RSH
487 enzymes. We confirm that, as was shown for H432E *E. coli* RelA mutant (Winther et al., 2018), the
488 corresponding H420E mutation in *B. subtilis* Rel is a useful tool for specifically abrogating activation
489 of Rel by starved ribosomal complexes. Additionally, we demonstrate the utility of two novel
490 mutations in the ZFD domain: R619E (R629E in *E. coli* RelA) as well as a double C602A/C603A
491 substitution (C612A/C613A in *E. coli* RelA). While these mutations do not completely abrogate the
492 activation, acting in epistasis they can be employed to reveal weaker phenotypes / effects, as it was
493 shown in the current work when the mutations were combined with RRM / ACT deletion.

494 Finally, we would like to draw the attention of the research community working on long RSH
495 enzymes to technical aspects of protein purification. It is common to purify Rel/RelA for biochemical
496 experiments using a single-step Ni-NTA purification (for example (Gratani et al., 2018;Wood et al.,
497 2019)). However, both RelA (Turnbull et al., 2019) and Rel have a strong tendency for RNA
498 contamination and multiple additional steps are necessary to remove this contaminant. Therefore,
499 reporting the 260/280 absorbance ratio of the final preparations is essential. RNA-free protein
500 preparations typically have a 260/280 absorbance ratio of 0.57, but this parameter can vary
501 depending on the amino acid composition, specifically the abundance of tryptophan and
502 phenylalanine (Layne, 1957). Without extra steps to remove RNA contamination, single-step
503 preparations are likely to be heavily RNA-contaminated. This contamination can potentially explain
504 the surprising observation that Ni-NTA purified *S. aureus* Rel inhibits the DEAD-box RNA helicase
505 CshA (Wood et al., 2019): the RNA contamination may be acting as a competitor in the CshA
506 helicase assay. RNA contamination also interferes with the estimate of the oligomerisation state of
507 Rel: since the RNA-bound protein elutes much earlier than the RNA-free (**Figure 2BC**). For
508 example, *Mycobacterium tuberculosis* Rel elutes as several peaks from SEC (Avarbock et al., 2005),
509 with the 'trimer' (i.e. RNA-contaminated) fraction having lower enzymatic activity. This is likely
510 because the RNA interferes with 'trimer' Rel activation by starved ribosomal complexes.

511 **5 References**

512 Agirrezabala, X., Fernandez, I.S., Kelley, A.C., Carton, D.G., Ramakrishnan, V., and Valle, M.
513 (2013). The ribosome triggers the stringent response by RelA via a highly distorted tRNA.
514 *EMBO Rep* 14**,** 811-816.

515 Akanuma, G., Kazo, Y., Tagami, K., Hiraoka, H., Yano, K., Suzuki, S., Hanai, R., Nanamiya, H.,
516 Kato-Yamada, Y., and Kawamura, F. (2016). Ribosome dimerization is essential for the
517 efficient regrowth of Bacillus subtilis. *Microbiology* 162**,** 448-458.

518 Antoun, A., Pavlov, M.Y., Tenson, T., and Ehrenberg, M.M. (2004). Ribosome formation from
519 subunits studied by stopped-flow and Rayleigh light scattering. *Biol Proced Online* 6**,** 35-54.

520 Arenz, S., Abdelshahid, M., Sohmen, D., Payoe, R., Starosta, A.L., Berninghausen, O., Hauryliuk,
521 V., Beckmann, R., and Wilson, D.N. (2016). The stringent factor RelA adopts an open
522 conformation on the ribosome to stimulate ppGpp synthesis. *Nucleic Acids Res* 44**,** 6471-
523 6481.

524 Atkinson, G.C., Tenson, T., and Hauryliuk, V. (2011). The RelA/SpoT homolog (RSH) superfamily:
525 distribution and functional evolution of ppGpp synthetases and hydrolases across the tree of
526 life. *PLoS One* 6**,** e23479.

527 Avarbock, A., Avarbock, D., Teh, J.S., Buckstein, M., Wang, Z.M., and Rubin, H. (2005). Functional
528 regulation of the opposing (p)ppGpp synthetase/hydrolase activities of RelMtb from
529 Mycobacterium tuberculosis. *Biochemistry* 44**,** 9913-9923.

530 Avarbock, D., Avarbock, A., and Rubin, H. (2000). Differential regulation of opposing RelMtb
531 activities by the aminoacylation state of a tRNA.ribosome.mRNA.RelMtb complex.
532 *Biochemistry* 39**,** 11640-11648.

533 Beljantseva, J., Kudrin, P., Andresen, L., Shingler, V., Atkinson, G.C., Tenson, T., and Hauryliuk, V.
534 (2017). Negative allosteric regulation of Enterococcus faecalis small alarmone synthetase
535 RelQ by single-stranded RNA. *Proc Natl Acad Sci U S A* 114**,** 3726-3731.

536 Block, H., Maertens, B., Spriestersbach, A., Brinker, N., Kubicek, J., Fabis, R., Labahn, J., and
537 Schafer, F. (2009). Immobilized-metal affinity chromatography (IMAC): a review. *Methods*
538 *Enzymol* 463**,** 439-473.

539 Boutte, C.C., and Crosson, S. (2011). The complex logic of stringent response regulation in
540 Caulobacter crescentus: starvation signalling in an oligotrophic environment. *Mol Microbiol*
541 80**,** 695-714.

542 Britton, R.A., Eichenberger, P., Gonzalez-Pastor, J.E., Fawcett, P., Monson, R., Losick, R., and
543 Grossman, A.D. (2002). Genome-wide analysis of the stationary-phase sigma factor (sigma-
544 H) regulon of Bacillus subtilis. *J Bacteriol* 184**,** 4881-4890.

545 Brodiazhenko, T., Johansson, M.J.O., Takada, H., Nissan, T., Hauryliuk, V., and Murina, V. (2018).
546 Elimination of Ribosome Inactivating Factors Improves the Efficiency of Bacillus subtilis and
547 Saccharomyces cerevisiae Cell-Free Translation Systems. *Front Microbiol* 9**,** 3041.

548 Brown, A., Fernandez, I.S., Gordiyenko, Y., and Ramakrishnan, V. (2016). Ribosome-dependent
549 activation of stringent control. *Nature* 534**,** 277-280.

550 Dalebroux, Z.D., Svensson, S.L., Gaynor, E.C., and Swanson, M.S. (2010). ppGpp conjures bacterial
551 virulence. *Microbiol Mol Biol Rev* 74**,** 171-199.

552 Dalebroux, Z.D., and Swanson, M.S. (2012). ppGpp: magic beyond RNA polymerase. *Nat Rev*
553 *Microbiol* 10**,** 203-212.

554 Geiger, T., Kastle, B., Gratani, F.L., Goerke, C., and Wolz, C. (2014). Two small (p)ppGpp
555 synthases in Staphylococcus aureus mediate tolerance against cell envelope stress conditions.
556 *J Bacteriol* 196**,** 894-902.

557 Golovanov, A.P., Hautbergue, G.M., Wilson, S.A., and Lian, L.Y. (2004). A simple method for
558 improving protein solubility and long-term stability. *J Am Chem Soc* 126**,** 8933-8939.

559 Gratani, F.L., Horvatek, P., Geiger, T., Borisova, M., Mayer, C., Grin, I., Wagner, S., Steinchen, W.,
560 Bange, G., Velic, A., Macek, B., and Wolz, C. (2018). Regulation of the opposing (p)ppGpp
561 synthetase and hydrolase activities in a bifunctional RelA/SpoT homologue from
562 Staphylococcus aureus. *PLoS Genet* 14**,** e1007514.

563 Gropp, M., Strausz, Y., Gross, M., and Glaser, G. (2001). Regulation of Escherichia coli RelA
564 requires oligomerization of the C-terminal domain. *J Bacteriol* 183**,** 570-579.

565 Haseltine, W.A., and Block, R. (1973). Synthesis of guanosine tetra- and pentaphosphate requires the
566 presence of a codon-specific, uncharged transfer ribonucleic acid in the acceptor site of
567 ribosomes. *Proc Natl Acad Sci U S A* 70**,** 1564-1568.

568 Hauryliuk, V., Atkinson, G.C., Murakami, K.S., Tenson, T., and Gerdes, K. (2015). Recent
569 functional insights into the role of (p)ppGpp in bacterial physiology. *Nat Rev Microbiol* 13**,**
570 298-309.

571 Inabe, T. (2005). Mellitate anions: unique anionic component with supramolecular self-organizing
572 properties. *Journal of Materials Chemistry* 15**,** 1317-1328.

573 Jiang, M., Sullivan, S.M., Wout, P.K., and Maddock, J.R. (2007). G-protein control of the ribosome-
574 associated stress response protein SpoT. *J Bacteriol* 189**,** 6140-6147.

575 Jimmy, S., Saha, C.K., Stavropoulos, C., Garcia-Pino, A., Hauryliuk, V., and Atkinson, G.C. (2019).
576 Discovery of small alarmone synthetases and their inhibitors as toxin-antitoxin loci. *bioXriv*
577 *[Preprint]***,** DOI: 10.1101/575399.

578 Kudrin, P., Dzhygyr, I., Ishiguro, K., Beljantseva, J., Maksimova, E., Oliveira, S.R.A., Varik, V.,
579 Payoe, R., Konevega, A.L., Tenson, T., Suzuki, T., and Hauryliuk, V. (2018). The ribosomal
580 A-site finger is crucial for binding and activation of the stringent factor RelA. *Nucleic Acids*
581 *Res* 46**,** 1973-1983.

582 Kudrin, P., Varik, V., Oliveira, S.R., Beljantseva, J., Del Peso Santos, T., Dzhygyr, I., Rejman, D.,
583 Cava, F., Tenson, T., and Hauryliuk, V. (2017). Subinhibitory Concentrations of
584 Bacteriostatic Antibiotics Induce relA-Dependent and relA-Independent Tolerance to beta-
585 Lactams. *Antimicrob Agents Chemother* 61.

586 Kushwaha, G.S., Bange, G., and Bhavesh, N.S. (2019). Interaction studies on bacterial stringent
587 response protein RelA with uncharged tRNA provide evidence for its prerequisite complex
588 for ribosome binding. *Curr Genet*.

589 Layne, E. (1957). Spectrophotometric and Turbidimetric Methods for Measuring Proteins. *Methods*
590 *in Enzymology* 3**,** 447-454.

591 Liu, K., Bittner, A.N., and Wang, J.D. (2015). Diversity in (p)ppGpp metabolism and effectors. *Curr*
592 *Opin Microbiol* 24**,** 72-79.

593 Loveland, A.B., Bah, E., Madireddy, R., Zhang, Y., Brilot, A.F., Grigorieff, N., and Korostelev, A.A.
594 (2016). Ribosome*RelA structures reveal the mechanism of stringent response activation.
595 *Elife* 5.

596 Mechold, U., Murphy, H., Brown, L., and Cashel, M. (2002). Intramolecular regulation of the
597 opposing (p)ppGpp catalytic activities of Rel(Seq), the Rel/Spo enzyme from Streptococcus
598 equisimilis. *J Bacteriol* 184**,** 2878-2888.

599 Mittenhuber, G. (2001). Comparative genomics and evolution of genes encoding bacterial (p)ppGpp
600 synthetases/hydrolases (the Rel, RelA and SpoT proteins). *J Mol Microbiol Biotechnol* 3**,**
601 585-600.

602 Molin, S., Stougaard, P., Uhlin, B.E., Gustafsson, P., and Nordstrom, K. (1979). Clustering of genes
603 involved in replication, copy number control, incompatibility, and stable maintenance of the
604 resistance plasmid R1drd-19. *J Bacteriol* 138**,** 70-79.

605 Murina, V., Kasari, M., Hauryliuk, V., and Atkinson, G.C. (2018a). Antibiotic resistance ABCF
606 proteins reset the peptidyl transferase centre of the ribosome to counter translational arrest.
607 *Nucleic Acids Res* 46**,** 3753-3763.

608 Murina, V., Kasari, M., Takada, H., Hinnu, M., Saha, C.K., Grimshaw, J.W., Seki, T., Reith, M.,
609 Putrins, M., Tenson, T., Strahl, H., Hauryliuk, V., and Atkinson, G.C. (2018b). ABCF
610 ATPases Involved in Protein Synthesis, Ribosome Assembly and Antibiotic Resistance:
611 Structural and Functional Diversification across the Tree of Life. *J Mol Biol*.

612 Nanamiya, H., Kasai, K., Nozawa, A., Yun, C.S., Narisawa, T., Murakami, K., Natori, Y.,
613 Kawamura, F., and Tozawa, Y. (2008). Identification and functional analysis of novel
614 (p)ppGpp synthetase genes in Bacillus subtilis. *Mol Microbiol* 67**,** 291-304.

615 Parker, J., Watson, R.J., and Friesen, J.D. (1976). A relaxed mutant with an altered ribosomal protein
616 L11. *Mol Gen Genet* 144**,** 111-114.

617 Ronneau, S., Caballero-Montes, J., Coppine, J., Mayard, A., Garcia-Pino, A., and Hallez, R. (2018).
618 Regulation of (p)ppGpp hydrolysis by a conserved archetypal regulatory domain. *Nucleic*
619 *Acids Res*.

620 Schreiber, G., Metzger, S., Aizenman, E., Roza, S., Cashel, M., and Glaser, G. (1991).
621 Overexpression of the relA gene in Escherichia coli. *J Biol Chem* 266**,** 3760-3767.

622 Shyp, V., Tankov, S., Ermakov, A., Kudrin, P., English, B.P., Ehrenberg, M., Tenson, T., Elf, J., and
623 Hauryliuk, V. (2012). Positive allosteric feedback regulation of the stringent response enzyme
624 RelA by its product. *EMBO Rep* 13**,** 835-839.

625 Spizizen, J. (1958). Transformation of Biochemically Deficient Strains of Bacillus Subtilis by
626 Deoxyribonucleate. *Proc Natl Acad Sci U S A* 44**,** 1072-1078.

627 Steinchen, W., and Bange, G. (2016). The magic dance of the alarmones (p)ppGpp. *Mol Microbiol*
628 101**,** 531-544.

629 Tagami, K., Nanamiya, H., Kazo, Y., Maehashi, M., Suzuki, S., Namba, E., Hoshiya, M., Hanai, R.,
630 Tozawa, Y., Morimoto, T., Ogasawara, N., Kageyama, Y., Ara, K., Ozaki, K., Yoshida, M.,
631 Kuroiwa, H., Kuroiwa, T., Ohashi, Y., and Kawamura, F. (2012). Expression of a small
632 (p)ppGpp synthetase, YwaC, in the (p)ppGpp(0) mutant of Bacillus subtilis triggers YvyD-
633 dependent dimerization of ribosome. *Microbiologyopen* 1**,** 115-134.

634 Tamman, H., Van Nerom, K., Takada, H., Vandenberk, S., Polikanov, Y., Hofkens, J., Talavera, A.,
635 Hauryliuk, V., Hendrix, J., and Garcia-Pino, A. (2019). Nucleotide-mediated allosteric
636 regulation of bifunctional Rel enzymes *bioRxiv*

637 Thomas, C.M., Hothersall, J., Willis, C.L., and Simpson, T.J. (2010). Resistance to and synthesis of
638 the antibiotic mupirocin. *Nat Rev Microbiol* 8**,** 281-289.

639 Turnbull, K.J., Dzhygyr, I., Lindemose, S., Hauryliuk, V., and Roghanian, M. (2019). Intramolecular
640 Interactions Dominate the Autoregulation of Escherichia coli Stringent Factor RelA. *Front*
641 *Microbiol* 10**,** 1966.

642 Van Nerom, K., Tamman, H., Takada, H., Hauryliuk, V., and Garcia-Pino, A. (2019). The Rel
643 stringent factor from Thermus thermophilus: crystallization and X-ray analysis. *Acta*
644 *Crystallogr F Struct Biol Commun* 75**,** 561-569.

645 Wendrich, T.M., Blaha, G., Wilson, D.N., Marahiel, M.A., and Nierhaus, K.H. (2002). Dissection of
646 the mechanism for the stringent factor RelA. *Mol Cell* 10**,** 779-788.

647 Wilkinson, R.C., Batten, L.E., Wells, N.J., Oyston, P.C., and Roach, P.L. (2015). Biochemical
648 studies on Francisella tularensis RelA in (p)ppGpp biosynthesis. *Biosci Rep* 35.

649 Winther, K.S., Roghanian, M., and Gerdes, K. (2018). Activation of the Stringent Response by
650 Loading of RelA-tRNA Complexes at the Ribosomal A-Site. *Mol Cell* 70**,** 95-105 e104.

651 Wood, A., Irving, S.E., Bennison, D.J., and Corrigan, R.M. (2019). The (p)ppGpp-binding GTPase
652 Era promotes rRNA processing and cold adaptation in Staphylococcus aureus. *PLoS Genet*
653 15**,** e1008346.

654 Xiao, H., Kalman, M., Ikehara, K., Zemel, S., Glaser, G., and Cashel, M. (1991). Residual guanosine
655 3',5'-bispyrophosphate synthetic activity of relA null mutants can be eliminated by spoT null
656 mutations. *J Biol Chem* 266**,** 5980-5990.

657 Yang, N., Xie, S., Tang, N.Y., Choi, M.Y., Wang, Y., and Watt, R.M. (2019). The Ps and Qs of
658 alarmone synthesis in Staphylococcus aureus. *PLoS One* 14**,** e0213630.

659 **6 Conflict of Interest**

660 *The authors declare that the research was conducted in the absence of any commercial or financial*
661 *relationships that could be construed as a potential conflict of interest*.

662 **7 Author Contributions**

663 HT conceived the study, HT, MR and VH designed experiments, HT performed experiments with *B.*
664 *subtilis* Rel, ID and MR performed experiments with *E. coli* RelA, RM and GA contributed tools and
665 reagents, GCA and AG-P performed structure and sequence analyses, HT and VH drafted and
666 revised the manuscript with contributions from MR, AG-P and GCA. All authors have read and
667 approved the final version of this manuscript.

668 **8 Funding**

669 This work was supported by the European Regional Development Fund through the Centre of
670 Excellence for Molecular Cell Technology (VH), the Molecular Infection Medicine Sweden (MIMS)
671 (VH), Swedish Research council (grant 2017-03783 to VH and grant 2015-04746 to GCA), Ragnar
672 Söderberg foundation (VH), Umeå Centre for Microbial Research (UCMR) (postdoctoral grant 2017
673 to HT), MIMS Excellence by Choice Postdoctoral Fellowship Programme (MR), the Fonds National
674 de Recherche Scientifique (grants FRFS-WELBIO CR-2017S-03, FNRS CDR J.0068.19 and FNRS-
675 PDR T.0066.18 to AG-P) and the Fonds Jean Brachet and the Fondation Van Buuren (AG-P).

676 **9 Acknowledgments**

677 We would like to thank the Protein Expertise Platform (PEP) at Umeå University and Mikael
678 Lindberg for constructing pET24d::*His*$_{10}$-*SUMO*-based expression constructs and purifying His$_6$-
679 Ulp1, and Julien Caballero-Montes for comments on the manuscript.

680 **10 Figures**

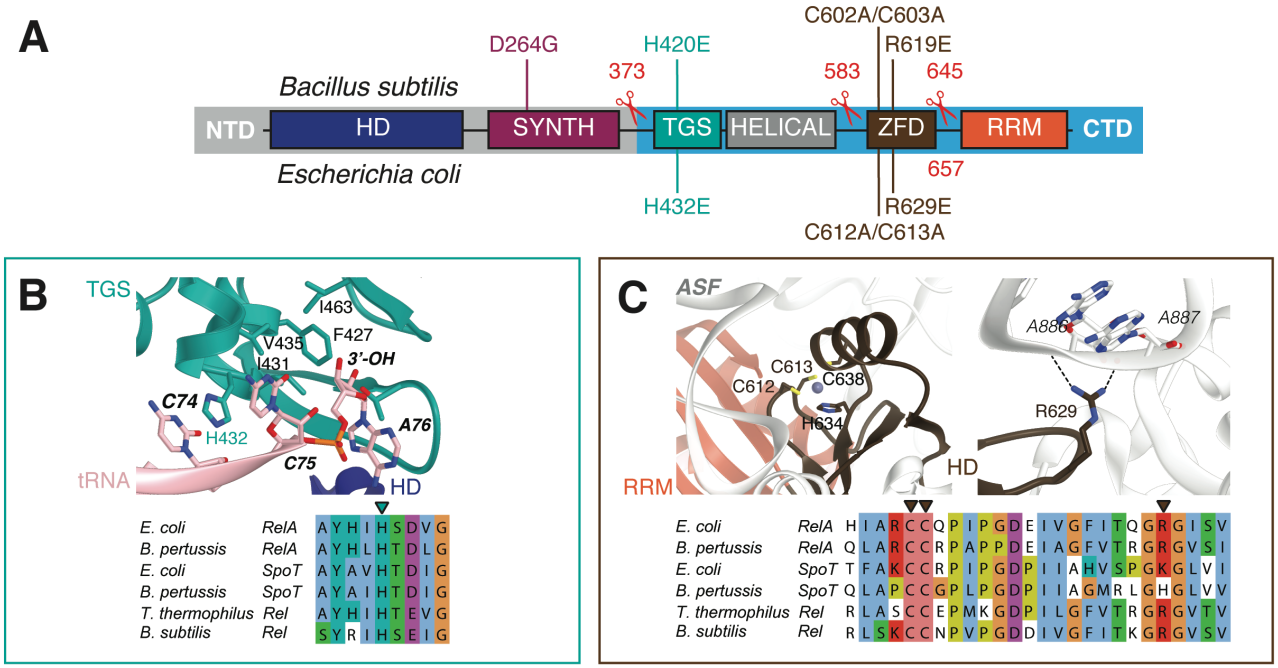

681

682 **Figure 1. Domain structure of 'long' ribosome-associated RSHs Rel and RelA.** (**A**) The NTD
683 region contains (p)ppGpp hydrolysis (HD) and (p)ppGpp synthesis (SYNTH) NTD domains. TGS
684 (ThrRS, GTPase and SpoT), Helical, ZFD (Zinc Finger Domain) and RRM (RNA Recognition
685 Motif) domains comprise the regulatory CTD region. Mutations and truncations of *B. subilis* Rel and
686 *E. coli* RelA used in this study are indicated above and below the domain schematics, respectively.
687 (**B**) Conservation and structural environment of mutations in the TGS domain used in the current
688 study. (**C**) Conservation and structural environment of mutations in the RRM domain used in the
689 current study. The 3D structures are as per from Loveland and colleagues (Loveland et al., 2016),
690 RDB accession number 5KPX.

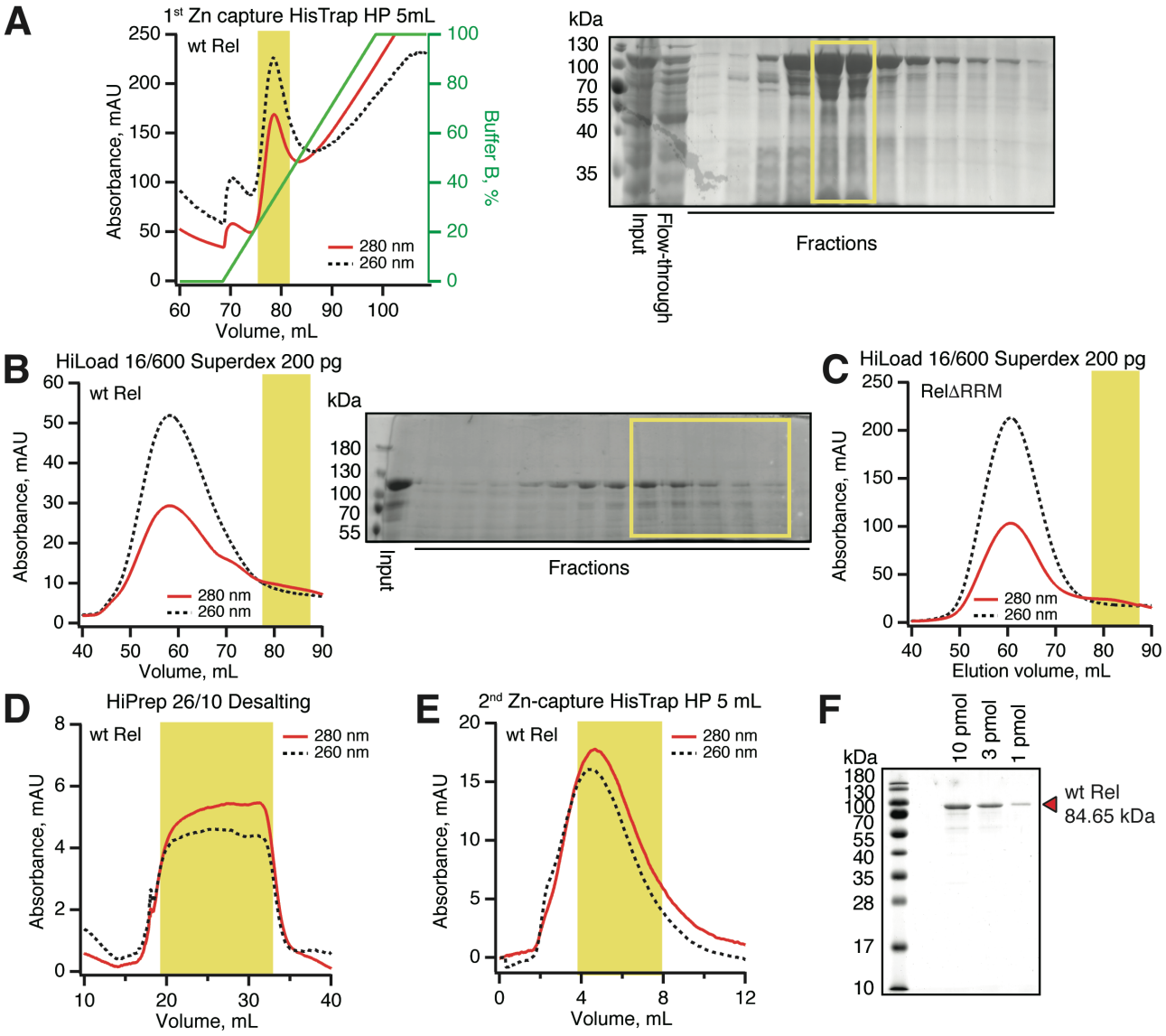

691

692 **Figure 2. Purification of RNA-free untagged *B. subtilis* Rel.** N-terminally His_{10}-SUMO tagged
693 RelA was overexpressed and purified as described in detail in *Materials and Methods*. (**A**) Cells were
694 lysed and subjected to immobilized metal affinity chromatography (IMAC) using Zn^{2+}-charged
695 HisTrap 5 mL HP column. The fraction corresponding the Rel with the lowest contamination of
696 nucleic acids (highlighted in yellow) was carried forward. Size-exclusion chromatography on HiLoad
697 16/600 Superdex 200 pg was used to further separate the RNA-free Rel fractions (**B**: full-length wild
698 type Rel; **C**: ΔRRM Rel). Following the buffer exchange on HiPrep 10/26 desalting column (**D**), the
699 boxed-out fractions were pooled and the His_{10}-SUMO tag was cleaved off by His_6-Ulp1 protease. (**E**)
700 His_6-Ulp1 and the His_{10}-SUMO tag was then purified from native untagged Rel by the second round
701 of IMAC. Highlighted fractions were pooled, concentrated, aliquoted, flash-frozen in liquid nitrogen
702 and stored –80 °C. (**F**) SDS-PAGE analysis of purified native untagged *B. subtilis* Rel.

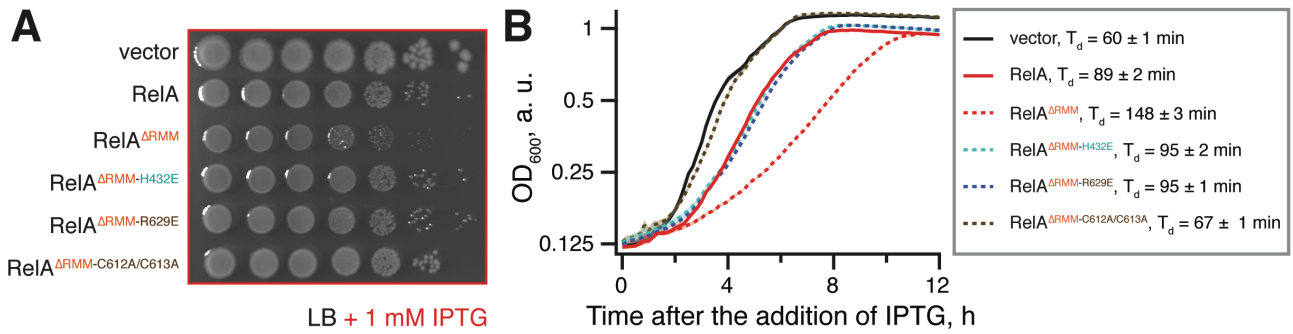

Figure 3. Toxicity of ΔRRM *E. coli* RelA is mitigated by mutations compromising interactions with tRNA and the ribosome. (**A**) *E. coli* BW25113 cells were transformed with low copy IPTG inducible vector pNDM220 (vector) or pNDM220-based constructs expressing wild-type and mutant versions of *E. coli* RelA as indicated on the figure. Ten-fold serial dilutions of overnight LB cultures were made and spotted onto LB agar (LA) supplemented with 30 µg/mL ampicillin and 1 mM IPTG. (**B**) Thousand-fold dilution of the same overnights were made in LB supplemented with 30 µg/mL ampicillin and 1 mM IPTG, and growth was at 37 °C was monitored using Bioscreen C growth curve analysis system. Doubling time (Td) was calculated from three independent measurements and the error bars represent standard errors.

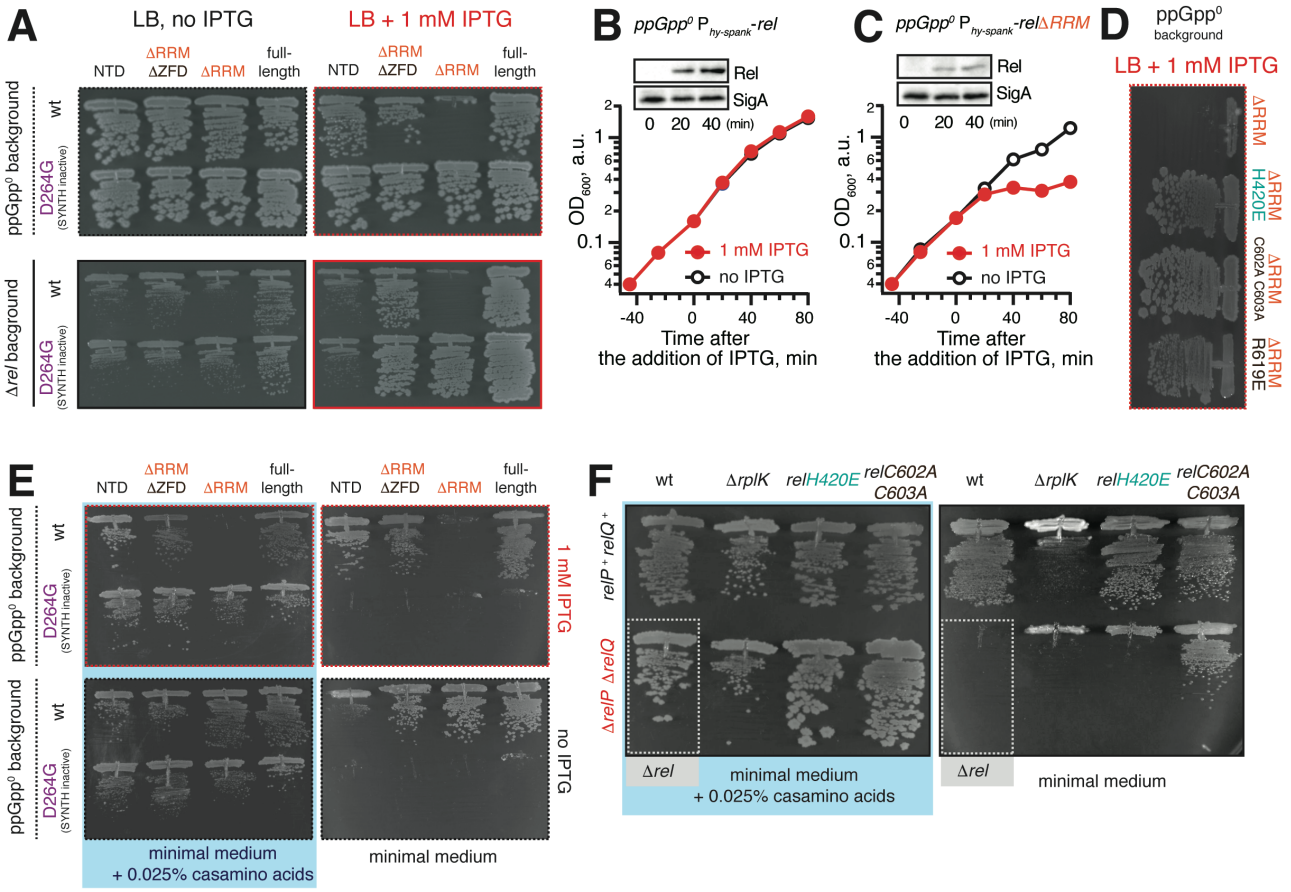

Figure 4. Deletion of the regulatory RRM domain leads to *B. subtilis* Rel toxicity due to ribosome-dependent (p)ppGpp overproduction. (**A**) Full-length (VHB155 and VHB183) as well as C-terminally truncated Rel variants [synthesis-competent ΔRRM (VHB159 and VHB184), ΔRRMΔZFD (VHB160 and VHB185) and Rel^{NTD} (VHB161 and VHB186), and the corresponding synthesis-inactive D264G mutants VHB162-164; VHB187-190] were expressed in either $ppGpp^0$ (test for toxicity mediated by (p)ppGpp accumulation) or Δ*rel* (test for HD functionality) *B. subtilis* growing on solid LB medium. Expression of $Rel^{\Delta RRM}$ causes growth defect in liquid culture. Either wild-type *rel* (VHB183) (**B**) or $rel^{\Delta RRM}$ mutant (VHB184) (**C**) were expressed in $ppGpp^0$ background grown in liquid LB medium at 37 °C. Protein expression was induced by IPTG added to final concentration of 1 mM to exponentially growing bacterial cultures at OD_{600} 0.2. Protein expression was monitored by Western blotting using anti-Rel antibodies. (**D**) Toxicity of mutant versions of $Rel^{\Delta RRM}$ tested in $ppGpp^0$ *B. subtilis* growing on solid LB medium: wild type $Rel^{\Delta RRM}$ (VHB184), H420E (VHB231) defective in recognition of tRNA's 3' CCA end, and ZFD mutants C602AC603A (VHB233) and R619E (VHB281) defective in 70S binding. LB plates were scored after 18 hour incubation at 37 °C. (**E**) Synthesis activity of Rel mutants probed by amino acid auxotrophy assays. *B. subtilis* strains were constructed using either $relP^+$ $relQ^+$ wild type 168 (upper row) or Δ*relP* Δ*relP* (lower row) background. The strains either expressed indicated *rel* mutants (H420E (VHB68) and C602A C603A (VHB148), upper row, and H420E (VHB60), C602A C603A (VHB62), lower row) or contained additional Δ*rplK* gene disruption (VHB47, $relP^+$ $relQ^+$ and VHB49, Δ*relP* Δ*relP*). The $ppGpp^0$ mutant strain (Δ*relP* Δ*relP* Δ*rel*, VHB63) was used as a control (highlighted with grey box). The strains were grown on either solid Spizizen minimal medium (right panel) or solid minimal medium supplemented with 0.025% casamino acids (left panel). (**F**) C-terminally truncated Rel variants (either synthesis-competent (VHB155, VHB159-161) or synthesis-inactive D264G mutant

737 versions (VHB156, VHB162-164)) were expressed in ppGpp^0 *B. subtilis* growing on either solid
738 minimal medium or solid minimal medium supplemented with 0.025% casamino acids. Plates were
739 scored after 36 hours incubation at 37 °C. Importantly, prior to experiment all strains were pre-
740 cultured on solid minimal medium supplemented with 0.025% casamino acids. This was done in
741 order avoid the effects caused by the decreased fitness of the inoculum.

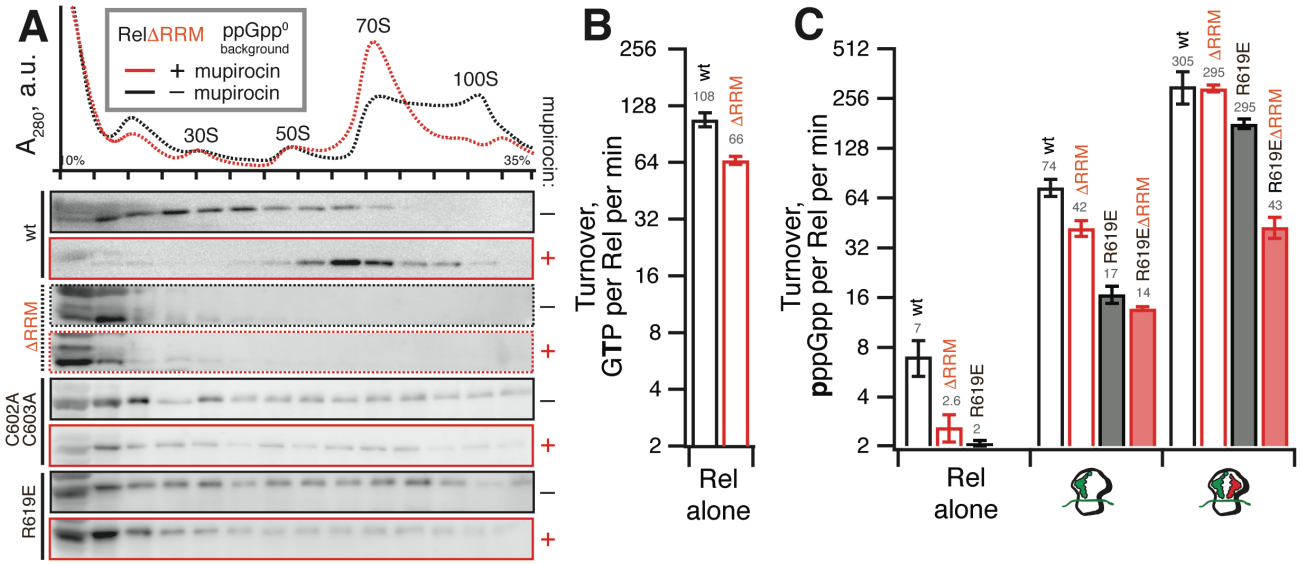

Figure 5. Deletion of the regulatory RRM domain destabilises Rel binding to starved ribosomal complexes and does not abrogate the hydrolysis activity. (**A**) Polysome profile and immunoblot analyses of Rel variants expressed either ectopically under the control of IPTG-inducible $P_{hy\text{-}spnak}$ promotor [ΔRRM Rel in ppGpp^0 *B. subtilis* (VHB184), R619E Rel in Δ*rel B. subtilis* (VHB282)] or from the native chromosomal locus [C602A C603A mutant (VHB144)]. Expression Rel$^{\Delta RRM}$ was induced by 1 mM IPTG for 10 minutes followed by a 10 minute challenge with 700 nM mupirocin. To drive the expression of RelR619E Rel the strain as grown in LB supplemented with 1 mM IPTG. In the case of R619E and C602AC603A Rel the culture was treated with mupirocin for 20 minutes. (**B**) Effect of the RRM deletion on Rel pppGpp-hydrolysis activity. (**C**) Effects of RRM deletion and R619E mutation on Rel synthetic activity either alone or in the presence of either initiation and starved ribosomal complexes. The error bars represent standard deviations of the turnover estimates by linear regression.